JOURNAL OF GUIDANCE, CONTROL, AND DYNAMICS
Vol. 23, No. 4, July–August 2000

Time-Explicit Representation of Relative Motion Between Elliptical Orbits

Robert G. Melton*
Pennsylvania State University, University Park, Pennsylvania 16802-1401

The classic treatment of rendezvous mechanics and other problems involving the relative motion of two spacecraft assumes a circular reference orbit, allowing a simple closed-form description of the motion. A solution is developed using an elliptical reference orbit, expanding the state transition matrix in powers of eccentricity, while retaining the explicit time dependence of the three-dimensional motion. The solution includes separate matrix elements for first- and second-order terms in eccentricity and for both Cartesian and cylindrical coordinates. Assessment of the maximum errors in position and velocity components over one complete revolution of the reference satellite shows that the solution is accurate for practical purposes with eccentricities in the range 0–0.3. An example application is given for the proposed laser interferometer space antenna gravity wave experiment.

Introduction

THE customary analysis of rendezvous mechanics begins with the linearized (Clohessy–Wiltshire) equations of motion[1,2] and assumes a circular reference orbit for the target vehicle, permitting a simple analytic description of the motion. Tschauner and Hempel[3] first solved the problem for motion relative to an elliptical orbit, but had to regularize the problem, resulting in a solution that does not explicitly include time. Other approaches by Lancaster[4] and Berreen and Sved[5] include the time dependence, but are limited to coplanar motion. Abrahamson and Stern[6] present a somewhat more general method that treats the problem for either elliptical or hyperbolic orbits. However, the solution is in terms of the eccentric and eccentric hyperbolic anomalies, so that one must still solve the Kepler problem to obtain the explicit time dependence for each particular application. More recent efforts by Kelly,[7] Garrison et al.,[8] Der and Danchick,[9] and Carter[10] provide representations of the three-dimensional relative motion, but all of these are functions of either the true or eccentric anomaly of one satellite. Solution of the Kepler problem is conceptually and numerically straightforward, but in instances where an onboard calculation of relative motion is required for estimation purposes, a direct, noniterative algorithm would be preferred. Further, a solution that depends solely on time as the independent variable can provide the same type of insight into the motion as do the Clohessy–Wiltshire equations.

This paper develops an approximate solution, accurate to order e^2, that explicitly includes time (and none of the angular anomalies) and that is valid for noncoplanar elliptical orbits.

Analysis

Consider two spacecraft in elliptical orbits (not necessarily coplanar) about a common gravitational source, as shown in Fig. 1. Employing the common designations associated with rendezvous mechanics, target vehicle denotes the spacecraft in the reference orbit, located at position $\boldsymbol{r}^*$, and chase vehicle denotes the second spacecraft, moving close to the target and with position $\boldsymbol{r}$. It is assumed for now that only a central gravitational source influences the motion and that the chase vehicle may experience an additional perturbing acceleration Γ. The equations of motion in Cartesian coordinates can be derived in a manner similar to that given in Refs. 1 and 2, although now the time dependence of the target orbit's radius and angular rate must be included. Using a coordinate system with the x axis aligned with the reference radius vector $\boldsymbol{r}^*$ and the z axis aligned with the target orbit's angular momentum vector, the equations of motion become

$$\ddot{x} = \frac{2\mu}{r^{*3}(t)}x + 2\omega(t)\dot{y} + \dot{\omega}(t)y + \omega^2(t)x + \Gamma_x(t) \tag{1a}$$

$$\ddot{y} = \frac{-\mu}{r^{*3}(t)}y - 2\omega(t)\dot{x} - \dot{\omega}(t)x + \omega^2(t)y + \Gamma_y(t) \tag{1b}$$

$$\ddot{z} = \frac{-\mu z}{r^{*3}(t)} + \Gamma_z(t) \tag{1c}$$

where μ is the gravitational parameter and ω the rotational rate of the x, y, z system. By forming the state vector $\delta\boldsymbol{x} = [\delta\boldsymbol{r}, \delta\boldsymbol{v}]^T$, where $\delta\boldsymbol{r} = \boldsymbol{r} - \boldsymbol{r}^*$ is the chase vehicle's relative position and $\delta\boldsymbol{v}$ is its relative velocity, the equations of motion can be written in matrix form as

$$\delta\dot{\boldsymbol{x}} = \boldsymbol{A}(t)\delta\boldsymbol{x} + \Gamma(t) \tag{2}$$

where

$$^R\boldsymbol{A}(t) = \begin{bmatrix} 0 & 0 & 0 & 1 & 0 & 0 \\ 0 & 0 & 0 & 0 & 1 & 0 \\ 0 & 0 & 0 & 0 & 0 & 1 \\ 2\mu/r^{*3} + \omega^2 & \dot{\omega} & 0 & 0 & 2\omega & 0 \\ -\dot{\omega} & -\mu/r^{*3} + \omega^2 & 0 & -2\omega & 0 & 0 \\ 0 & 0 & -\mu/r^{*3} & 0 & 0 & 0 \end{bmatrix} \tag{3}$$

$$^R\Gamma(t) = [0 \quad 0 \quad 0 \quad \Gamma_x \quad \Gamma_y \quad \Gamma_z]^T \tag{4}$$

where the superscript R denotes quantities expressed in rectangular (Cartesian) coordinates. Converting the formulation to cylindrical coordinates can potentially give a greater accuracy for large angular separations between spacecraft, but the preferred formulation depends on the form of the perturbing acceleration Γ. The cylindrical coordinates ρ, θ, and z are given by $\rho = x$, $\theta = y/r^*$, and $z = z$. In the case of a circular reference orbit, r^* is constant, requiring only appropriate changes to Eqs. (1a and 1b) and the corresponding elements of $\boldsymbol{A}$; however, for an elliptical reference orbit, Eqs. (1) and (3) become

$$\ddot{\rho} = (2\mu/r^{*3})\rho + 2\omega r^*\dot{\theta} + 2\omega\dot{r}^*\theta + \dot{\omega}r^*\theta + \omega^2\rho + \Gamma_\rho \tag{5a}$$

$$\ddot{\theta} = (1/r^*)\left(-\mu\theta/r^{*2} - 2\omega\dot{\rho} - \dot{\omega}\rho + \omega^2 r^*\theta - \ddot{r}^*\theta - 2\dot{r}^*\dot{\theta} + \Gamma_\theta\right) \tag{5b}$$

$$\ddot{z} = \frac{-\mu z}{r^{*3}(t)} + \Gamma_z(t) \tag{5c}$$

Received 8 June 1998; revision received 7 November 1999; accepted for publication 7 November 1999. Copyright © 1999 by Robert G. Melton. Published by the American Institute of Aeronautics and Astronautics, Inc., with permission.

*Associate Professor, Department of Aerospace Engineering, 233 Hammond Building; rgmelton@psu.edu. Associate Fellow AIAA.

$$
{}^{C}\boldsymbol{A}(t) = \begin{bmatrix}
0 & 0 & 0 & 1 & 0 & 0 \\
0 & 0 & 0 & 0 & 1 & 0 \\
0 & 0 & 0 & 0 & 0 & 1 \\
2\mu/r^{*3} + \omega^2 & \dot{\omega}r^* + 2\omega\dot{r}^* & 0 & 0 & 2\omega r^* & 0 \\
-\dot{\omega}/r^* & (1/r^*)(-\mu/r^{*2} + \omega^2 r^* - \ddot{r}^*) & 0 & -2\omega/r^* & -2\dot{r}^*/r^* & 0 \\
0 & 0 & -\mu/r^{*3} & 0 & 0 & 0
\end{bmatrix} \tag{6}
$$

where the superscript C denotes quantities expressed in the cylindrical coordinate system. The state vector for this system is $\delta\boldsymbol{x} = [\rho, \theta, z, \dot{\rho}, \dot{\theta}, \dot{z}]^T$.

Truncated approximations (to order e^2) for the time-varying terms in $\boldsymbol{A}(t)$ can be generated using Lagrange's generalized expansion theorem[11]:

$$r^*/a^* = 1 + e^2/2 - e\cos M^* - (e^2/2)\cos 2M^* + \mathcal{O}(e^3) \tag{7}$$

$$\omega = h^*/r^{*2} = (h^*/a^{*2})\{1 + 2e\cos M^* + (e^2/2)[5\cos 2M^* + 1] + \mathcal{O}(e^3)\} \tag{8}$$

$$\dot{\omega} = (-2h^*/r^{*3})\dot{r}^* = (-2h^*/a^{*2})\{en^*\sin M^* + e^2 n^*\sin 2M^* + 3e^2 n^*\cos M^*\sin M^* + \mathcal{O}(e^3)\} \tag{9}$$

$$\omega^2 = h^{*2}/r^{*4} = (h^{*2}/a^{*4})\{1 + 4e\cos M^* + e^2(3 + 7\cos 2M^*) + \mathcal{O}(e^3)\} \tag{10}$$

$$n^* = \sqrt{\mu/a^{*3}} \tag{11}$$

where $M^* = n^*(t - t_p)$ and t_p is the time of periapsis passage. The asterisk denotes quantities associated with the reference ellipse.

Formally, the solution to the homogeneous set is

$$\delta\boldsymbol{x}(t) = \Phi(t, 0)\delta\boldsymbol{x}(0) = \exp\left(\int \boldsymbol{A}(t)\,\mathrm{d}t\right)\delta\boldsymbol{x}(0) \tag{12}$$

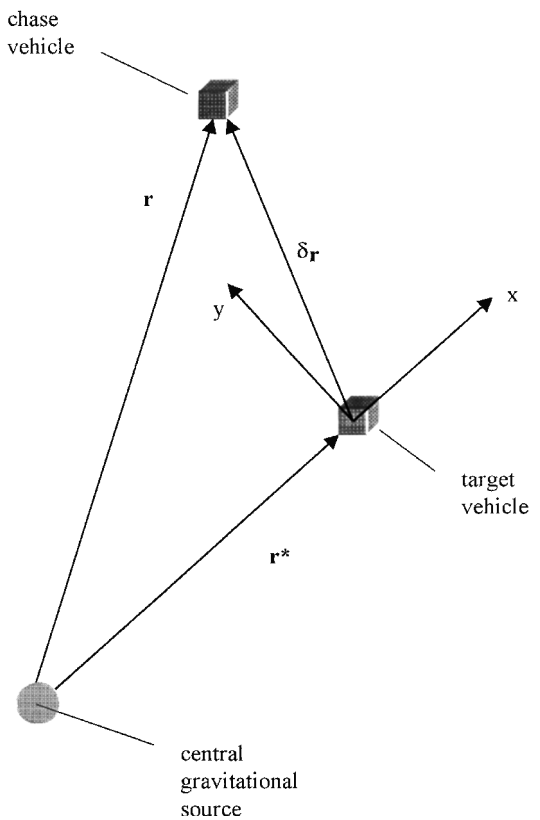

Fig. 1 Position of chase vehicle relative to target vehicle.

but the matrix exponential cannot be determined in closed form because of the time dependence of $\boldsymbol{A}$; however, $\boldsymbol{A}(t)$ is periodic and also can be expanded in terms of e as

$$\boldsymbol{A}(t) = \boldsymbol{A}_0 + e\boldsymbol{A}_1(t) + e^2\boldsymbol{A}_2(t) + \cdots \tag{13}$$

where $\boldsymbol{A}_0$ is the constant part of $\boldsymbol{A}(t)$. Therefore, according to a theorem by Poincaré (see Ref. 12) the state transition matrix can also be expanded as

$$\Phi(t, 0) = \Phi_0 + e\Phi_1(t) + e^2\Phi_2(t) + \cdots \tag{14}$$

where

$$\Phi_0 = \exp(\boldsymbol{A}_0 t) \tag{15}$$

Differentiating Eq. (14) yields

$$\frac{\mathrm{d}}{\mathrm{d}t}\Phi(t) = \boldsymbol{A}_0 e^{\boldsymbol{A}_0 t} + e\frac{\mathrm{d}\Phi_1}{\mathrm{d}t} + e^2\frac{\mathrm{d}^2\Phi_2}{\mathrm{d}t^2} + \cdots \tag{16}$$

Because the state transition matrix must also satisfy the homogeneous form of Eq. (2), then

$$\frac{\mathrm{d}}{\mathrm{d}t}\Phi(t) = \boldsymbol{A}(t)\Phi(t) = \left[\boldsymbol{A}_0 + e\boldsymbol{A}_1(t) + e^2\boldsymbol{A}_2(t) + \cdots\right] \times \left[e^{\boldsymbol{A}_0 t} + e\Phi_1(t) + \cdots\right] \tag{17}$$

Equating coefficients of like powers of e yields

$$\begin{aligned}
\frac{\mathrm{d}\Phi_1}{\mathrm{d}t} &= \boldsymbol{A}_0\Phi_1(t) + \boldsymbol{A}_1(t)e^{\boldsymbol{A}_0 t} \\
\frac{\mathrm{d}\Phi_2}{\mathrm{d}t} &= \boldsymbol{A}_0\Phi_2(t) + \boldsymbol{A}_1(t)\Phi_1(t) + \boldsymbol{A}_2(t)e^{\boldsymbol{A}_0 t} \\
&\vdots \\
\frac{\mathrm{d}\Phi_n}{\mathrm{d}t} &= \boldsymbol{A}_0\Phi_n(t) + \boldsymbol{A}_1(t)\Phi_{n-1}(t) + \cdots + \boldsymbol{A}_{n-1}(t)\Phi_1(t) + \boldsymbol{A}_n(t)e^{\boldsymbol{A}_0 t}
\end{aligned} \tag{18}$$

Because $\Phi(0) = \boldsymbol{I}$ and $\Phi_0(0) = \boldsymbol{I}$, it follows that for $\Phi_n(0) = 0$ for $n \geq 1$. Therefore, the expansion of $\Phi(t)$ can be determined recursively:

$$\begin{aligned}
\Phi_1(t) &= \int_0^t e^{\boldsymbol{A}_0(t-s)}\boldsymbol{A}_1(s)e^{\boldsymbol{A}_0 s}\,\mathrm{d}s \\
\Phi_2(t) &= \int_0^t e^{\boldsymbol{A}_0(t-s)}\left[\boldsymbol{A}_1(s)\Phi_1(s) + \boldsymbol{A}_2(s)e^{\boldsymbol{A}_0 s}\right]\mathrm{d}s \\
&\vdots \\
\Phi_n(t) &= \int_0^t e^{\boldsymbol{A}_0(t-s)}\left[\boldsymbol{A}_1(s)\Phi_{n-1}(s) + \cdots + \boldsymbol{A}_n(s)e^{\boldsymbol{A}_0 s}\right]\mathrm{d}s
\end{aligned} \tag{19}$$

Substituting Eqs. (7–11) into Eq. (3) and evaluating Eqs. (15) and (19) yield

$$
{}^{R}\Phi_0 = \begin{bmatrix}
4-3\cos nt & 0 & 0 & \sin nt/n & (2/n)(1-\cos nt) & 0 \\
6(\sin nt - nt) & 1 & 0 & -(2/n)(1-\cos nt) & (4\sin nt - 3nt)/n & 0 \\
0 & 0 & \cos nt & 0 & 0 & \sin nt/n \\
3n\sin nt & 0 & 0 & \cos nt & 2\sin nt & 0 \\
-6n(1-\cos nt) & 0 & 0 & -2\sin nt & 4\cos nt - 3 & 0 \\
0 & 0 & -n\sin nt & 0 & 0 & \cos nt
\end{bmatrix} \tag{20}
$$

(which is simply the state transition matrix for the case of a circular reference orbit) and also higher-order terms for the case of an elliptical reference orbit.

Generating these higher-order terms is a laborious task even with the assistance of symbolic manipulation software because these systems cannot automatically resolve ambiguities in integrating the complex-valued functions in Eqs. (19). Therefore, elements of ${}^{R}\Phi_1$ and ${}^{R}\Phi_2$ are provided in the Appendix (all expansions here include terms through order e^2). Repeating the procedure using Eq. (6) and carrying terms of $\mathcal{O}(e^2)$ give the state transition matrix expressed for cylindrical coordinates ${}^{C}\Phi(t)$; elements of this expansion also appear in the Appendix.

One notes the appearance of secular terms in the angular component of the solution (as expected because generally the periods of the two satellites will differ), but secular terms also appear in the higher-order radial components. Such terms also appear in Kelly's solution.[7] These clearly have no physical significance and must be accepted as artifacts of this type of expansion.

The additional forcing function $\Gamma(t)$ could be included via a convolution term:

$$
\delta\boldsymbol{x}(t) = \Phi(t)\delta\boldsymbol{x}(0) + \int_0^t \Phi(t-\tau)\Gamma(\tau)\,\mathrm{d}\tau \tag{21}
$$

In the situation where Γ is the spacecraft's thrust acceleration, the explicit time dependence poses no difficulty; however, if Γ is to include gravitational perturbations from other sources, some *a priori* time-dependent form of the perturbations would be required.

Accuracy of the Solution

In all of the example cases to be cited, the errors are calculated relative to numerical integrations of the exact equations of motion. That is, positions and velocities are calculated separately for the target (reference) and chase vehicles, and the differences in these quantities are compared with those estimated using the approximate solutions. Extensive numerical studies show that the series expansion Eqs. (14–19) converges rapidly to the solution of the linearized equations (1) and (5); however, these linearized equations can be poor representations of the actual orbital motion, for example, if the chase and target vehicles' states differ by more than a few percent, and the reader must be mindful of this limitation.

As expected, the formulation in cylindrical coordinates gives more accurate results for larger angular separations, that is, greater than 0.01 rad, and for an elliptical reference orbit this depends also on the true anomaly of the target vehicle. Although a complete depiction of sensitivity to initial conditions is not possible, the following example serves to demonstrate the performance of the solution. The examples in this paper employ a system of canonical units where the gravitational parameter $\mu = 4\pi^2$ and the unit of length is the reference orbit's semi-major axis length a, thus making the time unit equal to one period of the reference orbit.

Consider a reference orbit with eccentricity e and a chase orbit with initial (relative) conditions

$$
\begin{aligned}
\delta\rho &= 0.001, & \delta\dot{\rho} &= 0.001 \\
\delta\theta &= 0.020, & \delta\dot{\theta} &= 0.001 \\
\delta z &= 0.001, & \delta\dot{z} &= 0.001
\end{aligned} \tag{22}
$$

Figures 2a–2c and 3a–3c show the maximum absolute errors in position and velocity components that occur over one revolution of the target vehicle. The target orbit eccentricities include the range $0 \le e \le 0.3$. In each case, the target vehicle starts at periapsis ($t = t_p$)

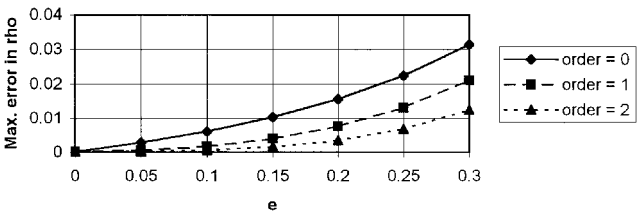

Fig. 2a Absolute error in radial position (canonical units).

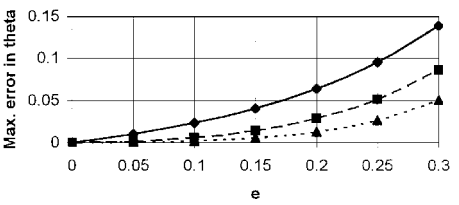

Fig. 2b Absolute error in angular position (canonical units).

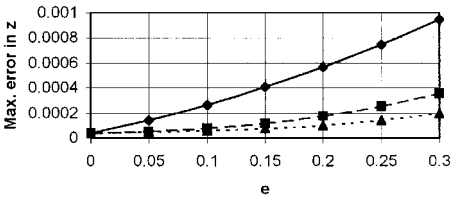

Fig. 2c Absolute error in out-of-plane position (canonical units).

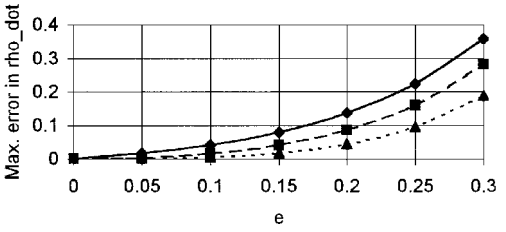

Fig. 3a Absolute error in radial rate (canonical units).

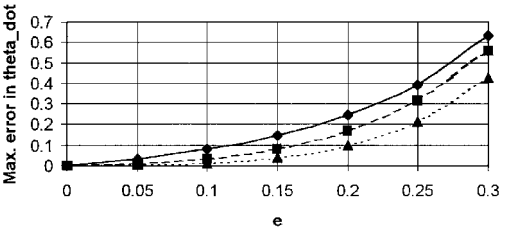

Fig. 3b Absolute error in angular rate (canonical units).

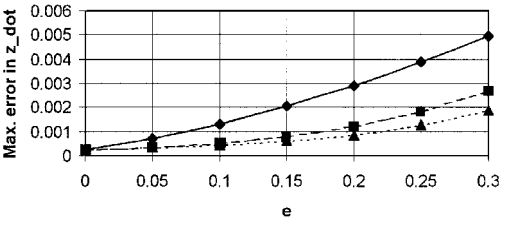

Fig. 3c Absolute error in out-of-plane rate (canonical units).

Table 1 Errors in range and range-rate for LISA orbits after 9 wk

Expansion order	Range error, %	Range-rate error, %
0	−1.5	−96
1	−1.3	−21
2	−1.3	−15

and the relative positions and rates are determined at 10,000 equally spaced time steps spanning one complete revolution of the target vehicle. These are compared with numerical integration of the individual vehicles' motions to compute the absolute errors. Clearly, including up through the first-order term in eccentricity adds significant accuracy even for low values of e; including the second-order terms becomes more important as the value of e becomes larger. In some applications (e.g., estimating rendezvous radar parameters or estimating intersatellite distances for interferometric studies), the individual components of position and their rates may not be as important as the range and range rate between spacecraft.

Application to the Laser Interferometer Space Antenna (LISA) Mission

The European Space Agency has proposed the laser interferometer space antenna (LISA) mission to detect and study low-frequency gravity waves. One potential configuration, proposed by Folkner et al.,[13,14] would place three spacecraft in heliocentric orbits with inclinations of approximately 0.96 deg, with eccentricities of approximately 0.00964, and with ascending nodes separated by 120 deg. Each spacecraft would be given the same true longitude on its own orbit, with the net effect being to create an equilateral triangle with the satellite pairs at the vertices and the interferometer arms forming the sides. This triangle, tilted 60 deg to the ecliptic plane, would allow the interferometer to naturally scan the cosmos for gravity waves, while maintaining an almost constant arm length (a necessity for the experiment) of approximately 5×10^6 km. Even in the absence of gravitational perturbations from Earth and other large planetary masses, the interferometer arms would not be precisely constant; further, any change in arm length of more than 7 mm/s could cause highly undesirable Doppler shifts in the interferometry. Control system design studies (anticipating the use of micro-Newton-level electric thrusters to compensate for disturbances) have shown the need for an analytic tool to estimate an arm length and its rate of change (range and range rate) for these orbits over an interval of 2–8 weeks. The method developed in this paper provides such a tool. Table 1 gives the errors for these estimates using the zero-, first- and second-order expansions. In cylindrical coordinates, the initial conditions for the relative motion of two ends of the interferometer arm are

$$\delta\rho = 0.0161543, \qquad \delta\dot{\rho} = -0.0255416$$

$$\delta\theta = -0.00850724, \qquad \delta\dot{\theta} = -0.204719$$

$$\delta z = 0.0279933, \qquad \delta\dot{z} = -0.0461563$$

Whereas there is little difference in accuracy for the range estimate, the range-rate approximation is substantially improved by addition of the first- and second-order terms. Note, however, that the range-rate error varies over the time interval 0–9 weeks, reaching values as high as 80%. Thus, use of this method for control-law selection should be restricted to identifying trends in the relative motion of the LISA satellites. Ongoing research is examining ways to include the effects of gravitational perturbations, as well as the control thrust, via the convolution integral of Eq. (21).

Conclusion

The approximate forms of the state transition matrix for rendezvous mechanics or other relative motion problems can be used with some confidence, with relatively small errors for reference orbits of small to moderate eccentricity ($0 < e < 0.3$); higher values of eccentricity may also be acceptable, but for much shorter time intervals. This solution also allows for the inclusion of other influences with an explicit time dependence, such as active thrusting. Whereas the overall accuracy is limited by the fidelity of the linearized gravity approximation, these state transition matrices provide a useful first approximation for mission planning purposes.

Appendix: Elements of the Expanded State Transition Matrix

To facilitate the labeling of matrix elements, the notation used here makes the expansion index a prefix, so that the kth term in Eq. (14) appears as ${}^{k}_{k}\Phi(t)$.

State Transition Matrix Elements: Rectangular Cartesian Coordinates

$$
\begin{aligned}
{}^{R}_{1}\Phi_{1,1} &= -5\cos[n(t-t_p)] - 3\cos[n(2t-t_p)] + 13\cos[nt_p] \\
&\quad - 5\cos[n(t+t_p)] - 6nt\sin[n(t-t_p)] \\
{}^{R}_{1}\Phi_{1,2} &= \sin[n(t-t_p)] + 2\sin[nt_p] - \sin[n(t+t_p)] \\
{}^{R}_{1}\Phi_{1.3} &= 0 \\
{}^{R}_{1}\Phi_{1,4} &= \{-3\sin[n(t-t_p)] + \sin[n(2t-t_p)] - 3\sin[nt_p] \\
&\quad + \sin[n(t+t_p)]\}/n \\
{}^{R}_{1}\Phi_{1,5} &= \{-\cos[n(t-t_p)] - 4\cos[n(2t-t_p)] + 8\cos[nt_p] \\
&\quad - 3\cos[n(t+t_p)] - 6nt\sin[n(t-t_p)]\}/(2n) \\
{}^{R}_{1}\Phi_{1,6} &= 0 \\
{}^{R}_{1}\Phi_{2,1} &= \{-12nt\cos[n(t-t_p)] - 30nt\cos[nt_p] + 4\sin[n(t-t_p)] \\
&\quad + 9\sin[n(2t-t_p)] - 7\sin[nt_p] + 20\sin[n(t+t_p)]\}/2 \\
{}^{R}_{1}\Phi_{2,2} &= \cos[n(t-t_p)] + \cos[nt_p] - 2\cos[n(t+t_p)] \\
&\quad - 3nt\sin[nt_p] \\
{}^{R}_{1}\Phi_{2,3} &= 0 \\
{}^{R}_{1}\Phi_{2,4} &= \{-8\cos[n(t-t_p)] + 3\cos[n(2t-t_p)] + \cos[nt_p] \\
&\quad + 4\cos[n(t+t_p)] + 6nt\sin[nt_p]\}/(2n) \\
{}^{R}_{1}\Phi_{2,5} &= -3\{nt\cos[n(t-t_p)] + nt\cos[nt_p] + \sin[n(t-t_p)] \\
&\quad - \sin[n(2t-t_p)] + \sin[nt_p] - \sin[n(t+t_p)]\}/n \\
{}^{R}_{1}\Phi_{2,6} &= 0, \qquad {}^{R}_{1}\Phi_{3,1} = 0, \qquad {}^{R}_{1}\Phi_{3,2} = 0 \\
{}^{R}_{1}\Phi_{3,3} &= \{\cos[n(2t-t_p)] - 3\cos[nt_p]\}/2 + \cos[n(t+t_p)] \\
{}^{R}_{1}\Phi_{3,4} &= 0, \qquad {}^{R}_{1}\Phi_{3,5} = 0 \\
{}^{R}_{1}\Phi_{3,6} &= \{-3\sin[n(t-t_p)] + \sin[n(2t-t_p)] - 3\sin[nt_p] \\
&\quad + \sin[n(t+t_p)]\}/(2n) \\
{}^{R}_{1}\Phi_{4,1} &= -n\{6nt\cos[n(t-t_p)] + \sin[n(t-t_p)] \\
&\quad - 6\sin[n(2t-t_p)] - 5\sin[n(t+t_p)]\} \\
{}^{R}_{1}\Phi_{4,2} &= n\{\cos[n(t-t_p)] - \cos[n(t+t_p)]\} \\
{}^{R}_{1}\Phi_{4,3} &= 0 \\
{}^{R}_{1}\Phi_{4,4} &= -3\cos[n(t-t_p)] + 2\cos[n(2t-t_p)] + \cos[n(t+t_p)] \\
{}^{R}_{1}\Phi_{4,5} &= \{-6nt\cos[n(t-t_p)] - 5\sin[n(t-t_p)] \\
&\quad + 8\sin[n(2t-t_p)] + 3\sin[n(t+t_p)]\}/2 \\
{}^{R}_{1}\Phi_{4,6} &= 0 \\
{}^{R}_{1}\Phi_{5,1} &= n\{-4\cos[n(t-t_p)] + 9\cos[n(2t-t_p)] - 15\cos[nt_p] \\
&\quad + 10\cos[n(t+t_p)] + 6nt\sin[n(t-t_p)]\}
\end{aligned}
$$

$$
\begin{aligned}
{}^{R}_{1}\Phi_{5,2} &= -n\{\sin[n(t-t_p)] + 3\sin[nt_p] - 2\sin[n(t+t_p)]\}\\
{}^{R}_{1}\Phi_{5,3} &= 0\\
{}^{R}_{1}\Phi_{5,4} &= 4\sin[n(t-t_p)] - 3\sin[n(2t-t_p)] + 3\sin[nt_p]\\
&\quad - 2\sin[n(t+t_p)]\\
{}^{R}_{1}\Phi_{5,5} &= 3\{-2\cos[n(t-t_p)] + 2\cos[n(2t-t_p)] - \cos[nt_p]\\
&\quad + \cos[n(t+t_p)] + nt\sin[n(t-t_p)]\}\\
{}^{R}_{1}\Phi_{5,6} &= 0, \qquad {}^{R}_{1}\Phi_{6,1} = 0, \qquad {}^{R}_{1}\Phi_{6,2} = 0\\
{}^{R}_{1}\Phi_{6,3} &= -n\{\sin[n(2t-t_p)] + \sin[n(t+t_p)]\}\\
{}^{R}_{1}\Phi_{6,4} &= 0, \qquad {}^{R}_{1}\Phi_{6,5} = 0\\
{}^{R}_{1}\Phi_{6,6} &= \{-3\cos[n(t-t_p)] + 2\cos[n(2t-t_p)]\\
&\quad + 3\cos[n(t+t_p)]\}/2\\
{}^{R}_{2}\Phi_{1,1} &= \{40 - 40\cos[2nt] - 40\cos[n(t-2t_p)]\\
&\quad - 27\cos[n(3t-2t_p)] - 24\cos[2n(t-t_p)] + 152\cos[2nt_p]\\
&\quad - 61\cos[n(t+2t_p)] - 60nt\sin[nt]\\
&\quad - 60nt\sin[(t-2t_p)] - 48nt\sin[2n(t-t_p)]\}/8\\
{}^{R}_{2}\Phi_{1,2} &= \{6nt\cos[nt] - 6nt\cos[n(t-2t_p)] + 2\sin[nt]\\
&\quad - 4\sin[2nt] + 7\sin[n(t-2t_p)] + 4\sin[2n(t-t_p)]\\
&\quad + 20\sin[2nt_p] - 9\sin[n(t+2t_p)]\}/4\\
{}^{R}_{2}\Phi_{1,3} &= 0\\
{}^{R}_{2}\Phi_{1,4} &= \{-12nt\cos[nt] + 12nt\cos[n(t-2t_p)] - 4\sin[nt]\\
&\quad + 8\sin[2nt] + 9\sin[n(3t-2t_p)] - 24\sin[2n(t-t_p)]\\
&\quad - 24\sin[2nt_p] + 9\sin[n(t+2t_p)]\}/(8n)\\
{}^{R}_{2}\Phi_{1,5} &= \{-6 + 12\cos[nt] - 6\cos[2nt] - \cos[n(t-2t_p)]\\
&\quad - 9\cos[n(3t-2t_p)] + 2\cos[2n(t-t_p)] + 14\cos[2nt_p]\\
&\quad - 6\cos[n(t+2t_p)] - 6nt\sin[nt] - 6nt\sin[n(t-2t_p)]\\
&\quad - 12nt\sin[2n(t-t_p)]\}/(4n)\\
{}^{R}_{2}\Phi_{1,6} &= 0\\
{}^{R}_{2}\Phi_{2,1} &= \{-30nt\cos[nt] - 30nt\cos[n(t-2t_p)]\\
&\quad - 24nt\cos[2n(t-t_p)] - 84nt\cos[2nt_p] - 30\sin[nt]\\
&\quad + 30\sin[2nt] + 11\sin[n(t-2t_p)] + 18\sin[n(3t-2t_p)]\\
&\quad + 6\sin[2n(t-t_p)] - 26\sin[2nt_p] + 61\sin[n(t+2t_p)]\}/4\\
{}^{R}_{2}\Phi_{2,2} &= \{-2 + 5\cos[nt] - 3\cos[2nt] + 2\cos[n(t-2t_p)]\\
&\quad + 2\cos[2n(t-t_p)] + 5\cos[2nt_p] - 9\cos[n(t+2t_p)]\\
&\quad - 3nt\sin[nt] + 3nt\sin[(t-2t_p)] - 12nt\sin[2nt_p]\}/2\\
{}^{R}_{2}\Phi_{2,3} &= 0\\
{}^{R}_{2}\Phi_{2,4} &= \{6 - 12\cos[nt] + 6\cos[2nt] + \cos[n(t-2t_p)]\\
&\quad + 6\cos[n(3t-2t_p)] - 14\cos[2n(t-t_p)] - 2\cos[2nt_p]\\
&\quad + 9\cos[n(t+2t_p)] + 6nt\sin[nt] - 6nt\sin[n(t-2t_p)]\\
&\quad + 12nt\sin[2nt_p]\}/(4n)\\
{}^{R}_{2}\Phi_{2,5} &= \{12nt - 6nt\cos[nt] - 6nt\cos[n(t-2t_p)]\\
&\quad - 12nt\cos[2n(t-t_p)] - 12nt\cos[2nt_p] - 24\sin[nt]\\
&\quad + 9\sin[2nt] + 12\sin[n(3t-2t_p)] - 9\sin[2n(t-t_p)]\\
&\quad - 9\sin[2nt_p] + 12\sin[n(t+2t_p)]\}/(4n)\\
{}^{R}_{2}\Phi_{2,6} &= 0, \qquad {}^{R}_{2}\Phi_{3,1} = 0, \qquad {}^{R}_{2}\Phi_{3,2} = 0\\
{}^{R}_{2}\Phi_{3,3} &= \{-4\cos[nt] + 4\cos[2nt] + 3\cos[n(3t-2t_p)]\\
&\quad - 12\cos[2nt_p] + 9\cos[n(t+2t_p)]\}/8\\
{}^{R}_{2}\Phi_{3,4} &= 0, \qquad {}^{R}_{2}\Phi_{3,5} = 0\\
{}^{R}_{2}\Phi_{3,6} &= \{-4\sin[nt] + 2\sin[2nt] + 3\sin[n(3t-2t_p)]\\
&\quad - 6\sin[2n(t-t_p)] - 6\sin[2nt_p] + 3\sin[n(t+2t_p)]\}/(8n)\\
{}^{R}_{2}\Phi_{4,1} &= n\{-60nt\cos[nt] - 60nt\cos[n(t-2t_p)]\\
&\quad - 96nt\cos[2n(t-t_p)] - 60\sin[nt] + 80\sin[2nt]\\
&\quad - 20\sin[n(t-2t_p)] + 81\sin[n(3t-2t_p)]\\
&\quad + 61\sin[n(t+2t_p)]\}/8\\
{}^{R}_{2}\Phi_{4,2} &= n\{8\cos[nt] - 8\cos[2nt] + \cos[n(t-2t_p)]\\
&\quad + 8\cos[2n(t-t_p)] - 9\cos[n(t+2t_p)]\\
&\quad - 6nt\sin[nt] + 6nt\sin[n(t-2t_p)]\}/4\\
{}^{R}_{2}\Phi_{4,3} &= 0\\
{}^{R}_{2}\Phi_{4,4} &= \{-16\cos[nt] + 16\cos[2nt] - 12\cos[n(t-2t_p)]\\
&\quad + 27\cos[n(3t-2t_p)] - 48\cos[2n(t-t_p)]\\
&\quad + 9\cos[n(t+2t_p)] + 12nt\sin[nt] - 12nt\sin[n(t-2t_p)]\}/8\\
{}^{R}_{2}\Phi_{4,5} &= \{-6nt\cos[nt] - 6nt\cos[n(t-2t_p)]\\
&\quad - 24nt\cos[2n(t-t_p)] - 18\sin[nt] + 12\sin[2nt]\\
&\quad - 5\sin[n(t-2t_p)] + 27\sin[n(3t-2t_p)] - 16\sin[2n(t-t_p)]\\
&\quad + 6\sin[n(t+2t_p)]\}/4\\
{}^{R}_{2}\Phi_{4,6} &= 0\\
{}^{R}_{2}\Phi_{5,1} &= n\{-60\cos[nt] + 60\cos[2nt] - 19\cos[n(t-2t_p)]\\
&\quad + 54\cos[n(3t-2t_p)] - 12\cos[2n(t-t_p)] - 84\cos[2nt_p]\\
&\quad + 61\cos[n(t+2t_p)] + 30nt\sin[nt] + 30nt\sin[n(t-2t_p)]\\
&\quad + 48nt\sin[2n(t-t_p)]\}/4\\
{}^{R}_{2}\Phi_{5,2} &= n\{-3nt\cos[nt] + 3nt\cos[n(t-2t_p)] - 8\sin[nt]\\
&\quad + 6\sin[2nt] + \sin[n(t-2t_p)] - 4\sin[2n(t-t_p)]\\
&\quad - 12\sin[2nt_p] + 9\sin[n(t+2t_p)]\}/2\\
{}^{R}_{2}\Phi_{5,3} &= 0\\
{}^{R}_{2}\Phi_{5,4} &= \{6nt\cos[nt] - 6nt\cos[n(t-2t_p)] + 18\sin[nt]\\
&\quad - 12\sin[2nt] - 7\sin[n(t-2t_p)] - 18\sin[n(3t-2t_p)]\\
&\quad + 28\sin[2n(t-t_p)] + 12\sin[2nt_p] - 9\sin[n(t+2t_p)]\}/4
\end{aligned}
$$

$$
\begin{aligned}
{}^{R}_{2}\Phi_{5,5} &= \{6 - 15\cos[nt] + 9\cos[2nt] - 3\cos[n(t-2t_p)] \\
&\quad + 18\cos[n(3t-2t_p)] - 15\cos[2n(t-t_p)] - 6\cos[2nt_p] \\
&\quad + 6\cos[n(t+2t_p)] + 3nt\sin[nt] + 3nt\sin[n(t-2t_p)] \\
&\quad + 12nt\sin[2n(t-t_p)]\}/2 \\
{}^{R}_{2}\Phi_{5,6} &= 0, \qquad {}^{R}_{2}\Phi_{6,1} = 0, \qquad {}^{R}_{2}\Phi_{6,2} = 0 \\
{}^{R}_{2}\Phi_{6,3} &= n\{4\sin[nt] - 8\sin[2nt] - 9\sin[n(3t-2t_p)] \\
&\quad - 9\sin[n(t+2t_p)]\}/8 \\
{}^{R}_{2}\Phi_{6,4} &= 0, \qquad {}^{R}_{2}\Phi_{6,5} = 0 \\
{}^{R}_{2}\Phi_{6,6} &= \{-4\cos[nt] + 4\cos[2nt] + 9\cos[n(3t-2t_p)] \\
&\quad - 12\cos[2n(t-t_p)] + 3\cos[n(t+2t_p)]\}/8
\end{aligned}
$$

State Transition Matrix Elements: Cylindrical Coordinates

The zeroth-order expansion in cylindrical coordinates ${}^{C}_{0}\Phi$ is identical to that in rectangular coordinates ${}^{R}_{0}\Phi$ except for the six elements

$$
\begin{aligned}
{}^{C}_{0}\Phi_{1,5} &= 2a(1-\cos[nt])/n, \qquad {}^{C}_{0}\Phi_{2,1} = (-6nt + \sin[nt])/a \\
{}^{C}_{0}\Phi_{2,4} &= -2(1-\cos[nt])/an, \qquad {}^{C}_{0}\Phi_{4,5} = 2a\sin[nt] \\
{}^{C}_{0}\Phi_{5,1} &= -6n(1-\cos[nt])/a, \qquad {}^{C}_{0}\Phi_{5,4} = -2\sin[nt]/a
\end{aligned}
$$

The first- and second-order expansions are as follows:

$$
\begin{aligned}
{}^{C}_{1}\Phi_{1,1} &= -5\cos[n(t-t_p)] - 3\cos[n(2t-t_p)] + 13\cos[nt_p] \\
&\quad - 5\cos[n(t+t_p)] - 6nt\sin[n(t-t_p)] \\
{}^{C}_{1}\Phi_{1,2} &= 0, \qquad {}^{C}_{1}\Phi_{1,3} = 0 \\
{}^{C}_{1}\Phi_{1,4} &= \{-3\sin[n(t-t_p)] + \sin[n(2t-t_p)] - 3\sin[nt_p] \\
&\quad + \sin[n(t+t_p)]\}/n \\
{}^{C}_{1}\Phi_{1,5} &= a\{\cos[n(t-t_p)] - 4\cos[n(2t-t_p)] + 4\cos[nt_p] \\
&\quad - \cos[n(t+t_p)] - 6nt\sin[n(t-t_p)]\}/(2n) \\
{}^{C}_{1}\Phi_{1,6} &= 0 \\
{}^{C}_{1}\Phi_{2,1} &= -\{24nt\cos[n(t-t_p)] + 30nt\cos[nt_p] - 4\sin[n(t-t_p)] \\
&\quad - 15\sin[n(2t-t_p)] + \sin[nt_p] - 20\sin[n(t+t_p)]\}/(2a) \\
{}^{C}_{1}\Phi_{2,2} &= 0, \qquad {}^{C}_{1}\Phi_{2,3} = 0 \\
{}^{C}_{1}\Phi_{2,4} &= \{-12\cos[n(t-t_p)] + 5\cos[n(2t-t_p)] + 3\cos[nt_p] \\
&\quad + 4\cos[n(t+t_p)] + 6nt\sin[nt_p]\}/(2an) \\
{}^{C}_{1}\Phi_{2,5} &= \{-6nt\cos[n(t-t_p)] - 5\sin[n(t-t_p)] + 5\sin[n(2t-t_p)] \\
&\quad - \sin[nt_p] + \sin[n(t+t_p)]\}/n \\
{}^{C}_{1}\Phi_{2,6} &= 0, \qquad {}^{C}_{1}\Phi_{3,1} = 0, \qquad {}^{C}_{1}\Phi_{3,2} = 0 \\
{}^{C}_{1}\Phi_{3,3} &= \tfrac{1}{2}\cos[n(2t-t_p)] - \tfrac{3}{2}\cos[nt_p] + \cos[n(t+t_p)] \\
{}^{C}_{1}\Phi_{3,4} &= 0, \qquad {}^{C}_{1}\Phi_{3,5} = 0 \\
{}^{C}_{1}\Phi_{3,6} &= \{-3\sin[n(t-t_p)] + \sin[n(2t-t_p)] \\
&\quad - 3\sin[nt_p] + \sin[n(t+t_p)]\}/(2n) \\
{}^{C}_{1}\Phi_{4,1} &= -n\{6nt\cos[n(t-t_p)] + \sin[n(t-t_p)] \\
&\quad - 6\sin[n(2t-t_p)] - 5\sin[n(t+t_p)]\} \\
{}^{C}_{1}\Phi_{4,2} &= 0, \qquad {}^{C}_{1}\Phi_{4,3} = 0 \\
{}^{C}_{1}\Phi_{4,4} &= -3\cos[n(t-t_p)] + 2\cos[n(2t-t_p)] + \cos[n(t+t_p)] \\
{}^{C}_{1}\Phi_{4,5} &= -a\{6nt\cos[n(t-t_p)] + 7\sin[n(t-t_p)] \\
&\quad - 8\sin[n(2t-t_p)] - \sin[n(t+t_p)]\}/2 \\
{}^{C}_{1}\Phi_{4,6} &= 0 \\
{}^{C}_{1}\Phi_{5,1} &= n\{-10\cos[n(t-t_p)] + 15\cos[n(2t-t_p)] \\
&\quad - 15\cos[nt_p] + 10\cos[n(t+t_p)] + 12nt\sin[n(t-t_p)]\}/a \\
{}^{C}_{1}\Phi_{5,2} &= 0, \qquad {}^{C}_{1}\Phi_{5,3} = 0 \\
{}^{C}_{1}\Phi_{5,4} &= \{6\sin[n(t-t_p)] - 5\sin[n(2t-t_p)] + 3\sin[nt_p] \\
&\quad - 2\sin[n(t+t_p)]\}/a \\
{}^{C}_{1}\Phi_{5,5} &= -11\cos[n(t-t_p)] + 10\cos[n(2t-t_p)] \\
&\quad + \cos[n(t+t_p)] + 6nt\sin[n(t-t_p)] \\
{}^{C}_{1}\Phi_{5,6} &= 0, \qquad {}^{C}_{1}\Phi_{6,1} = 0, \qquad {}^{C}_{1}\Phi_{6,2} = 0 \\
{}^{C}_{1}\Phi_{6,3} &= -n\{\sin[n(2t-t_p)] + \sin[n(t+t_p)]\} \\
{}^{C}_{1}\Phi_{6,4} &= 0, \qquad {}^{C}_{1}\Phi_{6,5} = 0 \\
{}^{C}_{1}\Phi_{6,6} &= \{-3\cos[n(t-t_p)] + 2\cos[n(2t-t_p)] \\
&\quad + \cos[n(t+t_p)]\}/2 \\
{}^{C}_{2}\Phi_{1,1} &= \{40 - 40\cos[2nt] - 40\cos[n(t-2t_p)] \\
&\quad - 27\cos[n(3t-2t_p)] - 24\cos[2n(t-t_p)] \\
&\quad + 152\cos[2nt_p] - 61\cos[n(t+2t_p)] - 60nt\sin[nt] \\
&\quad - 60nt\sin[n(t-2t_p)] - 48nt\sin[2n(t-t_p)]\}/8 \\
{}^{C}_{2}\Phi_{1,2} &= 0, \qquad {}^{C}_{2}\Phi_{1,3} = 0 \\
{}^{C}_{2}\Phi_{1,4} &= \{-12nt\cos[nt] + 12nt\cos[n(t-2t_p)] - 4\sin[nt] \\
&\quad + 8\sin[2nt] + 9\sin[n(3t-2t_p)] - 24\sin[2n(t-t_p)] \\
&\quad - 24\sin[2nt_p] + 9\sin[n(t+2t_p)]\}/(8n) \\
{}^{C}_{2}\Phi_{1,5} &= a\{-10 + 12\cos[nt] - 2\cos[2nt] + 2\cos[n(t-2t_p)] \\
&\quad - 9\cos[n(3t-2t_p)] + 6\cos[2n(t-t_p)] + 2\cos[2nt_p] \\
&\quad - \cos[n(t+2t_p)] - 12nt\sin[2n(t-t_p)]\}/(4n) \\
{}^{C}_{2}\Phi_{1,6} &= 0 \\
{}^{C}_{2}\Phi_{2,1} &= \{-12nt - 60nt\cos[nt] - 60nt\cos[n(t-2t_p)] \\
&\quad - 60nt\cos[2n(t-t_p)] - 84nt\cos[2nt_p] - 28\sin[nt] \\
&\quad + 50\sin[2nt] + 6\sin[n(t-2t_p)] + 39\sin[n(3t-2t_p)] \\
&\quad + 10\sin[2n(t-t_p)] - 6\sin[2nt_p] + 61\sin[n(t+2t_p)]\}/(4a) \\
{}^{C}_{2}\Phi_{2,2} &= 0, \qquad {}^{C}_{2}\Phi_{2,3} = 0 \\
{}^{C}_{2}\Phi_{2,4} &= \{-2 - 8\cos[nt] + 10\cos[2nt] + 6\cos[n(t-2t_p)] \\
&\quad + 13\cos[n(3t-2t_p)] - 30\cos[2n(t-t_p)] + 2\cos[2nt_p] \\
&\quad + 9\cos[n(t+2t_p)] + 12nt\sin[nt] - 12nt\sin[n(t-2t_p)] \\
&\quad + 12nt\sin[2nt_p]\}/(4an)
\end{aligned}
$$

$$
{}^{C}_{2}\Phi_{2,5} = \{6nt - 30nt\cos[2n(t-t_p)] - 16\sin[nt] + 5\sin[2nt] + 26\sin[n(3t-2t_p)] - 25\sin[2n(t-t_p)] - \sin[2nt_p]\} + 2\sin[n(t+2t_p)]/(4n)
$$

$$
{}^{C}_{2}\Phi_{2,6} = 0, \qquad {}^{C}_{2}\Phi_{3,1} = 0, \qquad {}^{C}_{2}\Phi_{3,2} = 0
$$

$$
{}^{C}_{2}\Phi_{3,3} = \{-4\cos[nt] + 4\cos[2nt] + 3\cos[n(3t-2t_p)] - 12\cos[2nt_p] + 9\cos[n(t+2t_p)]\}/8
$$

$$
{}^{C}_{2}\Phi_{3,4} = 0, \qquad {}^{C}_{2}\Phi_{3,5} = 0
$$

$$
{}^{C}_{2}\Phi_{3,6} = \{-4\sin[nt] + 2\sin[2nt] + 3\sin[n(3t-2t_p)] - 6\sin[2n(t-t_p)] - 6\sin[2nt_p] + 3\sin[n(t+2t_p)]\}/(8n)
$$

$$
{}^{C}_{2}\Phi_{4,1} = n\{-60nt\cos[nt] - 60nt\cos[n(t-2t_p)] - 96nt\cos[2n(t-t_p)] - 60\sin[nt] + 80\sin[2nt] - 20\sin[n(t-2t_p) + 81\sin[n(3t-2t_p)] + 61\sin[n(t+2t_p)]\}/8
$$

$$
{}^{C}_{2}\Phi_{4,2} = 0, \qquad {}^{C}_{2}\Phi_{4,3} = 0
$$

$$
{}^{C}_{2}\Phi_{4,4} = \{-16\cos[nt] + 16\cos[2nt] + 12\cos[n(t-2t_p)] + 27\cos[n(3t-2t_p)] - 48\cos[2n(t-t_p)] + 9\cos[n(t+2t_p)] + 12nt\sin[nt] - 12nt\sin[n(t-2t_p)]\}/8
$$

$$
{}^{C}_{2}\Phi_{4,5} = -a\{24nt\cos[2n(t-t_p)] + 12\sin[nt] - 4\sin[2nt] + 2\sin[n(t-2t_p)] - 27\sin[n(3t-2t_p)] + 24\sin[2n(t-t_p)] - \sin[n(t+2t_p)]\}/4
$$

$$
{}^{C}_{2}\Phi_{4,6} = 0
$$

$$
{}^{C}_{2}\Phi_{5,1} = n\{-12 - 88\cos[nt] + 100\cos[2nt] - 54\cos[n(t-2t_p)] + 117\cos[n(3t-2t_p)] - 40\cos[2n(t-t_p)] - 84\cos[2nt_p] + 61\cos[n(t+2t_p)] + 60nt\sin[nt] + 60nt\sin[n(t-2t_p)] + 120nt\sin[2n(t-t_p)]\}/(4a)
$$

$$
{}^{C}_{2}\Phi_{5,2} = 0, \qquad {}^{C}_{2}\Phi_{5,3} = 0
$$

$$
{}^{C}_{2}\Phi_{5,4} = \{12nt\cos[nt] - 12nt\cos[n(t-2t_p)] + 20\sin[nt] - 20\sin[2nt] - 18\sin[n(t-2t_p)] - 39\sin[n(3t-2t_p)] + 60\sin[2n(t-t_p)] + 12\sin[2nt_p] - 9\sin[n(t+2t_p)]\}/(4a)
$$

$$
{}^{C}_{2}\Phi_{5,5} = \{3 - 8\cos[nt] + 5\cos[2nt] + 39\cos[n(3t-2t_p)] - 40\cos[2n(t-t_p)] + \cos[n(t+2t_p)] + 30nt\sin[2n(t-t_p)]\}/2
$$

$$
{}^{C}_{2}\Phi_{5,6} = 0, \qquad {}^{C}_{2}\Phi_{6,1} = 0 \qquad {}^{C}_{2}\Phi_{6,2} = 0
$$

$$
{}^{C}_{2}\Phi_{6,3} = n\{4\sin[nt] - 8\sin[2nt] - 9\sin[n(3t-2t_p)] - 9\sin[n(t+2t_p)]\}/8
$$

$$
{}^{C}_{2}\Phi_{6,4} = 0, \qquad {}^{C}_{2}\Phi_{6,5} = 0
$$

$$
{}^{C}_{2}\Phi_{6,6} = \{-4\cos[nt] + 4\cos[2nt] + 9\cos[n(3t-2t_p)] - 12\cos[2n(t-t_p)] + 3\cos[n(t+2t_p)]\}/8
$$

Acknowledgments

I gratefully acknowledge the Rutherford Appleton Laboratory, where this work was conducted. I wish to thank Yusuf Jafry at the European Space Research and Technology Center for suggesting this problem in conjunction with the proposed laser interferometer space antenna mission and Jean Kechichian, with The Aerospace Corporation, for providing useful comments on the manuscript.

References

[1]Prussing, J. E., and Conway, B. A., *Orbital Mechanics*, Oxford Univ. Press, Oxford, England, U.K., 1993, Chap. 8.

[2]Wiesel, W. E., *Spaceflight Dynamics*, 2nd ed., McGraw–Hill, New York, 1997, pp. 80–85.

[3]Tschauner, J., and Hempel, P., "Rendezvous with a Target in an Elliptical Orbit," *Astronautica Acta*, Vol. 11, No. 2, 1965, pp. 104–109.

[4]Lancaster, E. R., "Relative Motion of Two Particles in Co-Planar Elliptic Orbits," *AIAA Journal*, Vol. 8, No. 10, 1970, pp. 1878, 1879.

[5]Berreen, T., and Sved, G., "Relative Motion of Particles in Coplanar Elliptic Orbits," *Journal of Guidance and Control*, Vol. 2, No. 5, 1979, pp. 443–446.

[6]Abrahamson, L. P., and Stern, R. G., "Two-Body Linear Guidance Matrices," Experimental Astronomy Lab. Rept. RE-14, Massachusetts Inst. of Technology, Cambridge, MA, March 1965.

[7]Kelly, T. J., "An Analytical Approach to the Two-Impulse Optimal Rendezvous Problem," *Advances in the Astronautical Sciences*, Vol. 87, 1994, pp. 337–347.

[8]Garrison, J. L., Gardner, T. G., and Axelrad, P., "Relative Motion in Highly Elliptical Orbits," *Advances in the Astronautical Sciences*, Vol. 89, 1995, pp. 1359–1376.

[9]Der, G., and Danchick, R., "An Analytic Approach to Optimal Rendezvous Using the Der–Danchick Equations," *Advances in the Astronautical Sciences*, Vol. 97, 1997, pp. 719–738.

[10]Carter, T. E., "State Transition Martrices for Terminal Rendezvous Studies: Brief Survey and New Example," *Journal of Guidance, Control, and Dynamics*, Vol. 21, No. 1, 1998, pp. 148–155.

[11]Battin, R. H., *An Introduction to the Mathematics and Methods of Astrodynamics*, AIAA Education Series, 1987, AIAA, Washington, DC, pp. 199–202.

[12]Reinhard, H., *Differential Equations: Foundations and Applications*, North Oxford Academic, London, 1986, pp. 451–457.

[13]Folkner, W. M., Hechler, F., Sweetser, T. H., Vincent, M. A., and Bender, P. L., "LISA Orbit Selection and Stability," *Proceedings of the First International LISA Symposium*, Rutherford Appleton Lab., Chilton, England, UK, 1996.

[14]Folkner, W. M., Bender, P. L., and Stebbins, R. T., "LISA Mission Concept Study: Laser Interferometer Space Antenna for the Detection and Observation of Gravitational Waves," Jet Propulsion Lab., JPL 97-16, California Inst. of Technology, Pasadena, CA, March 2, 1998.